

Replay to the review of: “Time dependent, non-monotonic response of warm convective cloud fields to changes in aerosol loading”

Dear Patrick,

Thank you so much for taking the time and reviewing our paper. It is not trivial that editor takes the lead and invests the time to carefully review a paper. We appreciate it. Your comments indeed helped us improving the clarity of the paper. We believe that after the additional clarifications and the modifications, the presented results are much clearer.

Specifically you highlighted the results presented in Figure 2 of the paper. As you’ll see in the detailed reply section below, there is no mistake in the figure. There are two reasons for the differences between the numbers we are showing to the ones in Lee et al, (2012). In Lee et al, you show a domain average for all voxels. Here we wanted to show the aerosol effect on the cloudy voxels only. We show that aerosols amplify both the evaporation and condensation processes in the polluted runs. Sometimes, there is a cancelation of the overall effect (condensation-evaporation) and so the net numbers are much smaller but the effect that the diffusion processes are enhanced means that the dynamic can be enhanced as well and so many other feedbacks. In our paper we averaged for cloudy voxels only, separately for supersaturation (condensation) and subsaturation (evaporation). As a sanity check we averaged as in Lee et al, and got similar results. Following this comment we have changed the figure and added explanations to make our results clearer.

Below please find detailed point-by-point answers to all of your comments. Please note that in the answers we present 3 types of figures. Figures that appear in the main text (numbered as Fig. x), figures that appear in the supporting information file (SI - numbered as Fig. Sx) and figures that appear only in this reply (numbered as Fig. Rx).

Lines 46-49: How do you define condensation or evaporation efficiency? Is it a column-integrated value? Later on (line 262) you reference Pinsky et al. 2013 and Seiki and Nakajima 2014, but in neither paper does the word “efficiency” actually appear. Do these papers use a different term? Are these really appropriate references if the term “condensation efficiency” does not appear? Koren et al. 2014 mentions

efficiency once but does not define the term. Please define this term carefully at some point, as you use it in various parts of the manuscript.

Answer: Thank you for highlighting this point. The condensation efficiency is related to the characteristic time scale of condensation (or evaporation) discussed in the provided references. As shown in Fig. 3 in Pinsky et al. (2013) and in Fig. 1 in Seiki and Nakajima (2014) the characteristic time scale of condensation (or evaporation) depends negatively on the cloud droplet number concentration. It means that under polluted conditions for a given supersaturation (subsaturation) the condensation (evaporation) will be faster. In other words, under polluted conditions the supersaturation will be consumed faster and more efficiently, increasing the latent heat release and invigorating the cloud development. To make it clearer we added a clarification to the revised manuscript:

"Under given supersaturation conditions, the condensation in polluted clouds is more efficient (higher condensation rate or shorter consumption time of the supersaturation - Pinsky et al., 2013; Seiki and Nakajima, 2014; Koren et al., 2014; Kogan and Martin, 1994; Dagan et al., 2015a)."

154-157: This doesn't very well describe how this manuscript is different from the numerous previous studies. Please make this clear.

Answer: Following this comment we have changed this part in the revised manuscript: *"In this work we explore the coupled microphysical-dynamic system of warm marine cloud fields using a bin-microphysics scheme under a large range of aerosol concentrations. We study the aerosol-cloud-environmental thermodynamic system by examining how changes in aerosol concentrations affect clouds properties, the related modifications of the thermodynamic conditions over time which as well drive feedbacks on the clouds' properties evolution."*

170-171: Only 2 hrs for spin-up? Lee et al. 2012 (in their Fig. 1; note: I was a co-author on this paper) shows 4 to 6 hrs was necessary for their case. Are you sure these

simulations are properly spun-up? Also, do the simulations include a diurnal cycle? Or is it fixed sun zenith angle? Or is it night time?

Answer: In order to better understand the complex interplay between microphysics, cloud dynamics and the derived evolution of the environmental thermodynamic conditions we preferred to simplify the system and to focus on idealized cases without including interactive radiative effects. Radiative cooling and changes of the SST due to changes in short wave radiation would be very important for marine stratocumulus cases for which the cloud fraction is large and therefore the radiative component is a key player. However, here since the average cloud fraction is low (~15%) and in order to separate coupled competing processes, the aerosol effects on the evolution of the thermodynamic properties were considered only by their effects via clouds. The radiative effects are prescribed and included in the large scale forcing (LSF - see table R1 below). To make this point clearer we added clarification to the methodology part of the revised manuscript: *“In order to focus on the aerosol effect on the thermodynamic properties of the field, the radiative effects (as included in the large scale forcing see details in Dagan et al., 2016) were prescribed in all simulations”*.

As for the spin-up time, the figures below present the time evolution of the total liquid water mass in the domain (Fig. R1a) and the domain mean liquid water center of gravity height (COG, Fig. R1b) for four different simulations differ by aerosol concentrations. After less than 2 hours of simulation the initial increase in these values desists and the difference between the simulations becomes significant. We note that other BOMEX studies (e.g. (Xue and Feingold, 2006;Jiang et al., 2006;Grabowski, 2014), and other trade Cu case studies (Xue et al., 2008;Seifert et al., 2015) used 2 h as the spin-up time. Following this comment we added a clarification to the revised manuscript: *“After 2 h of simulations the initial increase in the total liquid water mass in the domain desisted and the differences between the simulations (differ by the aerosol loading) became significant. Therefore 2h is determined as spin-up time (similar to the spin-up time in Xue and Feingold, 2006).”*

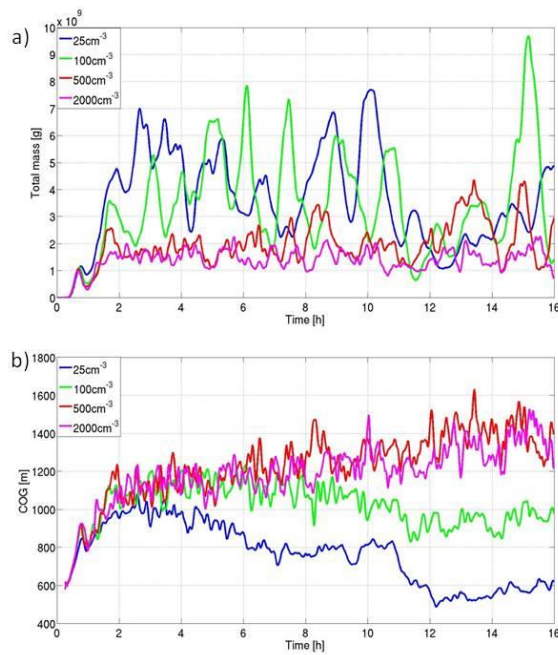


Figure R1. Evolution of (a) Total liquid water mass and (b) liquid water center of gravity for four different simulations differ by the aerosol loading.

Table R1. The large-scale forcing (LSF) standard setup used for the BOMEX case study simulations. The LSF includes temperature, water vapor mixing ratio and vertical velocity tendencies as a function of height.

Z [m]	Temperature tendency by LSF [K/s]	Water vapor mixing ratio tendency by LSF [kg/kg s]	Vertical velocity tendency by LSF [m/s]
0	$-2.315 \cdot 10^{-5}$	$-1.2 \cdot 10^{-8}$	0
300	$-2.315 \cdot 10^{-5}$	$-1.2 \cdot 10^{-8}$	-0.0013
500	$-2.315 \cdot 10^{-5}$	0	-0.0021
1500	$-2.315 \cdot 10^{-5}$	0	-0.065
2100	$-1.389 \cdot 10^{-5}$	0	0
2500	0	0	0

175: So what is the fixed shaped of the aerosol size distribution? “based on...” is not particularly enlightening.

Answer: The aerosol size distribution used in this work is a marine aerosol size distribution, which was published in Jaenicke 1988 and was described in Altaratz et al., 2008, as well. We give details in the text about the method we used to change the concentration but keep the size distribution similar. To make it clearer we changed this sentence in the revised manuscript: *"The aerosol distribution adopts a marine size distribution (see details in Jaenicke 1988 and Altaratz et al., 2008). Eight different simulations were conducted simulating a wide range of aerosol loading conditions from extremely pristine to polluted (total concentration of: 5, 25, 50, 100, 250, 500, 2000 and 5000 cm⁻³ near ground level, Dagan et al., 2015a). To reduce the results sensitivity to the shape of the aerosol size distribution and to focus on the aerosol number concentration effect, the different aerosol concentrations are calculated by multiplication of all bins by a constant factor and maintaining a similar shape of the size distribution."*

178: Some of these values are really very small. Are they really applicable to the atmosphere? (Also see comment regarding line 200 about adding Nd to Fig 1).

Answer: Thank you for this comment. On the same note of our answer regarding the radiative effects, we think that using ideal conditions helps gaining better process level understanding and factor separation. Some of the assumptions are not common in nature (concentration of 5 cm⁻³ is indeed super pristine). However, learning how the system will react to the extreme clean (or polluted) conditions helps constraining competition between processes. Moreover, some of the systems sensitivities to aerosol concentration are of logarithmic nature in which changes from super pristine to slightly polluted can yield the clearest aerosol signal, which can later be explored for the whole aerosol spectrum.

We added to the revised text: *"Eight different simulations were conducted simulating a wide range of aerosol loading conditions from extremely pristine to polluted (total*

concentration of: 5, 25, 50, 100, 250, 500, 2000 and 5000 cm^{-3} near ground level, Dagan et al., 2015a).”

184-185: I'm confused by the fact that the aerosol “maintains constant mixing ratio with height” but simultaneously “a prognostic eqn is solved for the aerosol mass”. If aerosol mass can appear because of, say, cloud drop evaporation, how can aerosol mass mixing ratio be constant with height? If aerosol size distributions are held constant, this is of course not physically realistic... what are the consequences for interpreting these results in the context of the real atmosphere?

Answer: Indeed our description was not clear enough. Only on the initialization stage of the simulation the aerosol mixing ratio is setup as constant with height. Once the simulation starts running the prognostic aerosol equation determines the aerosol mixing ratio at each voxel. To make this point clearer we added clarification to the revised manuscript: *"The aerosol is assumed to be composed of ammonium-sulfate and initialized with constant mixing ratio with height. A prognostic equation is solved for the aerosol mass, including regeneration upon evaporation and removal by surface rain."*

189: Is Khain et al. 2000 a reference to Kohler theory, or a scheme to calculate activation? If the former, that seems like a poor choice.

Answer: the aerosol activation scheme we used is described in Khain et al. 2000 and is based on the Kohler theory. In the revised text we added: *"The aerosol serves as potential cloud condensation nuclei (CCN) and it is activated based on the Kohler theory (the scheme is described in Khain et al., 2000)."*

200: Analyzing the data in this way supposes that there's no overall tendency in time. Is this true? If not, what is the tendency relative to the de-trended variability? How would the results change if a different time window (say, 8 hrs instead of 14) were analyzed?

Answer: This question is answered on the next section of the paper. As first order view (in section 3.1) we calculate the mean cloud field properties for the entire

simulation time. In the following section (3.2) we divide the simulations to shorter time windows and examine the trends with time (please see Fig. 6 in the manuscript). We added a clarification sentence about it: "*The aerosol effects on the mean field properties during the entire run are examined first following by a more detailed examination of the time evolution in the next section*".

200: Please add a panel showing mean drop concentration.

Answer: based on the previous reviewers' comments we added information regarding the mean drop concentration and size to the supporting information (SI). Since our paper is already loaded with text and figures, we preferred to leave it in the SI.

The reference to it in the main text: "*The effects of changes in aerosol concentration on the drop concentration and its mean size, for the different simulations can be found in Fig. S1 in the supporting information (SI)*."

The information provided in the SI:

"S.1 Mean size and number of drops

Figure S1 presents vertical profiles of the mean concentration and mean drop size per height. It demonstrates that at the cloudy layer ($H > 500\text{m}$) the mean drop size decreases with aerosol loading, while its concentration increases (Twomey, 1977). Below cloud base the trend is reversed – larger rain drops and lower concentration under more polluted conditions (similar to what was shown in Altaratz et al., 2008).

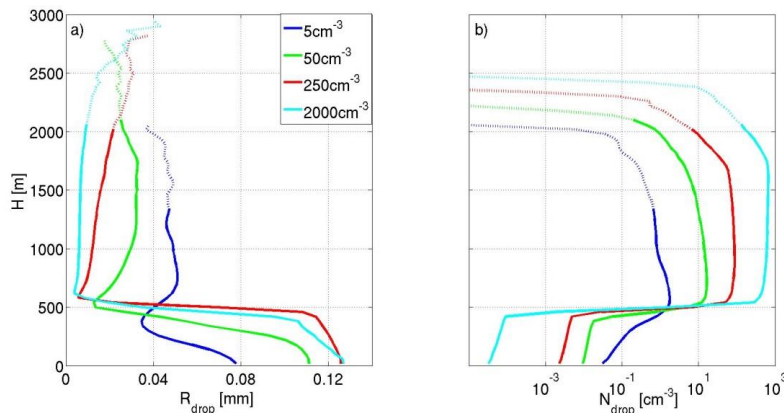


Figure S1. Vertical profiles of a) the mean (over time and domain) drop radius, and b) the mean (over the second two hours of simulation - after the spin-up time) of drop maximum concentration. These results include both cloud and raindrops for four simulations (with aerosol loading levels of 5 cm^{-3} – blue, 50 cm^{-3} – green, 250 cm^{-3} – red, and 2000 cm^{-3} – cyan). Dotted parts of the curves represent heights in which the total liquid water mass was less than 1% of the maximum total mass (Fig. 4b) to avoid conclusions based on small statistics."

200: What is the number of clouds in any given simulation? Does it change with aerosol number? Perhaps add this as a separate panel to Fig. 1.

Answer: recent studies showed that the number of clouds in the domain increases with the aerosol loading (Heiblum et al., 2016; Seigel, 2014). The small amount of clouds under clean conditions is a result of clustering of the clouds under precipitating conditions (Seifert and Heus, 2013). This trend is also true in our simulations (see (Heiblum et al., 2016) which is based on the same set of simulations). Nevertheless, it was also shown that in order to fully capture the organization pattern one must simulate a larger domain (Seifert and Heus, 2013) which is beyond our current computational abilities (using bin microphysical scheme). This limitation is mentioned in the main text: "Due to computational limitations, we had to restrict the

domain size to a scale that has a limited capability for capturing large scale organization (Seifert and Heus, 2013)."

Because of this limitation and because it was the focus of a few recent studies (some of which are mentioned above) we prefer not to focus on warm cumulus organization and its reflection on the total cloud number in this study.

218: Choosing the maximum value of any parameter seems very prone to outliers. Could you instead plot the, say, 90th or 95th percentile cloud top height to tell the same story?

Answer: We agree that maximum values can be sometimes prone to outliers. In our case however, we present the mean over time of the maximum cloud top height. This averaging is based on 1 minute time series over 14 hours (840 values) and hence possible contribution of outliers is averaged out. Moreover, we present in Figures 1 and 6 both the maximum and the mean cloud top height. We believe that both of them together capture, in the best way, the cloud fields' mean properties response to changes in aerosol loading (together with the total cloud mass, LWC and CF).

Moreover, the maximum cloud top height is a predictor of the cloud deepening effect over time (which is discussed in section 3.2). The size distribution of the clouds contains many small clouds and only few large ones, which contribute to the evaporation at the inversion layer and the subsequent deepening of the cloudy layer. Those clouds are really at the tail of the distribution and hence we prefer to keep the maximum cloud top.

To show that the 90th percentile cloud top height demonstrates the same general trend (both for the mean over the entire simulation time and for the evolution in time as presented in Fig. 6 of the main text) we present it here as well (Fig R2).

We have added clarification to the revised manuscript: *"Presenting together the mean over time of the maximum and the mean cloud top height captures, in a compact, yet informative, way the response of the clouds top height distribution in the domain to changes in aerosol loading and reduces the sensitivity to outliers. Moreover, by averaging over time we decreased the significance of the outliers as well."*

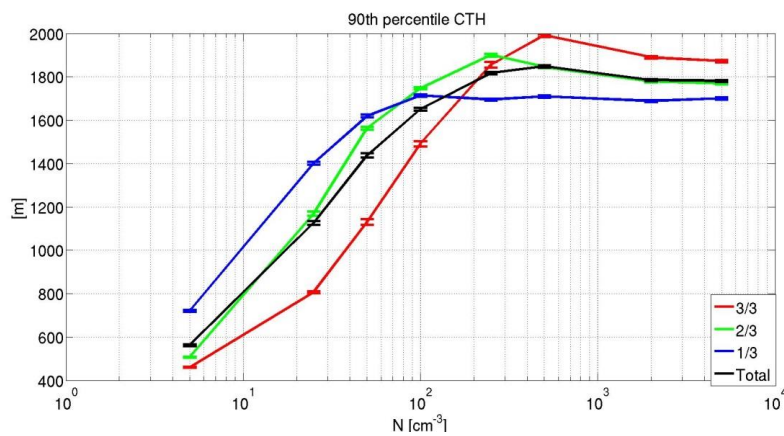


Figure R2. The 90th percentile cloud top height (CTH) as a function of the aerosol concentration used in the simulation. In addition to the total (black curve) it is calculated separately for each period of one third of the simulations (blue, green and red for the first, second and third periods, respectively). The error bars present the standard error.

242: I don't understand Fig 2. Lee et al. 2012 shows values between NET condensation of clean and polluted simulations to be on the order of 0.1 to 1 g/kg/day, which is about $1e-6$ to $1e-5$ g/kg/s. You show (gross) values that are as much as 4 orders of magnitude larger. These are not compatible. I think something is very wrong with your plot.

Answer: Thank you for this comment that helped us clarifying the paper's findings. There is no contradiction between the two results. The reason for the differences between Lee et al. (2012) and our results is the averaging method. As in many cases there is a choice whether to average for the entire domain that includes mostly voids (in the case of trade Cu) or to average for cloudy pixels only. Moreover, one can present the total condensation-evaporation balance, or since both are measurable and take place in other voxels in the cloud, one can present both condensation and evaporation rates, separately. Lee et al. (2012) presented the domain's mean net condensation evaporation while we present separately the mean gross values for the rate of condensation and evaporation for cloudy voxels only. We used this method of averaging to emphasis the increase in both condensation (in the supersaturated areas in the domain) and evaporation (in the subsaturated areas in the domain) rates with

aerosol loading, despite the decrease in cloud fraction (as can be seen in Fig. 1C in the main text and Fig. R4 below). Figure R3 below presents the mean values (over space and time) of net condensation rate for our simulations (using the same averaging method as performed in Lee et al. 2012) and indeed its order of magnitude is $1e-5$ g/kg/s. The small differences between Lee et al. (2012) and our results can be probably attributed to the different case study simulated (RICO vs BOMEX) and to the different microphysical scheme.

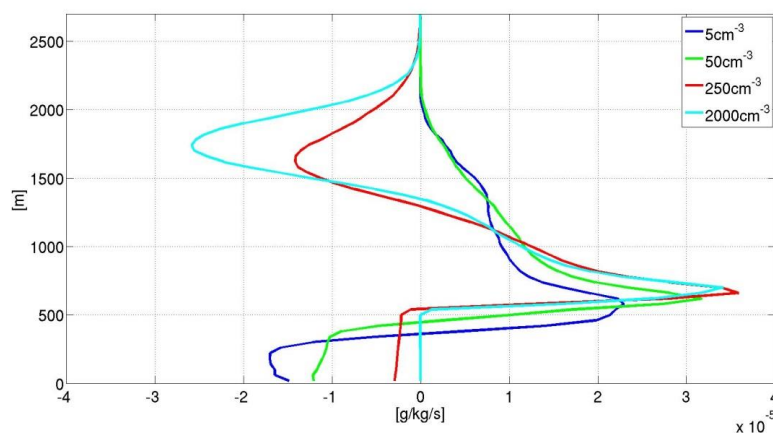


Figure R3: Domain's mean net condensation-less-evaporation tendencies for four different aerosol loading levels (5 cm^{-3} – blue, 50 cm^{-3} – green, 250 cm^{-3} – red, and 2000 cm^{-3} – cyan).

Following this comment and to avoid confusion we have moved the original Fig. 2 into the SI (as it supports our claim of an increase in both condensation and evaporation rates with aerosol loading) and now we present an alternative figure in the main text (please see below) that shows the vertical profiles of the total condensation and evaporation mass for the different simulations.

The changes done accordingly in the revised manuscript: “Fig. 2 presents the vertical profiles of the total condensation and evaporation mass during the simulations, for four different simulations. We note that as the aerosol loading increases, both the

condensed and evaporated mass increased (this is due to the increase in the diffusion rates – see Fig. S2, SI, and despite the decrease in cloud fraction – see Fig. 1C, Dagan et al., 2015a; Koren et al., 2014; Pinsky et al., 2013; Seiki and Nakajima, 2014). Below cloud base (located around 550 m) the clean simulations have small rain evaporation values which is absent in the polluted simulations."

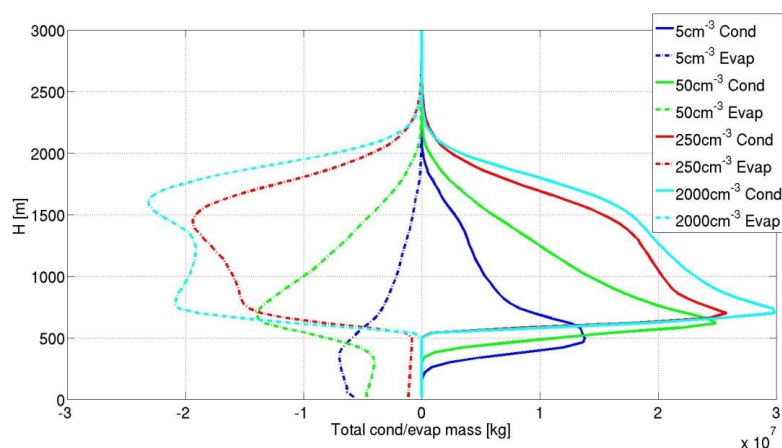


Figure 2 (the revised version). Domain's total condensed (solid lines) and evaporated mass (dashed lines) for 14 hours of simulation along four different simulations conducted with different aerosol concentration levels (5 cm^{-3} blue, 50 cm^{-3} green, 250 cm^{-3} red and 2000 cm^{-3} cyan).

The additions to the SI:

"S.2 Mean condensation and evaporation rates

Figure S2 presents vertical profiles of the mean (over time) of the condensation and evaporation rates, per height, for four simulations with different aerosol loading. It demonstrates the increase in both condensation and evaporation rates with aerosol loading.

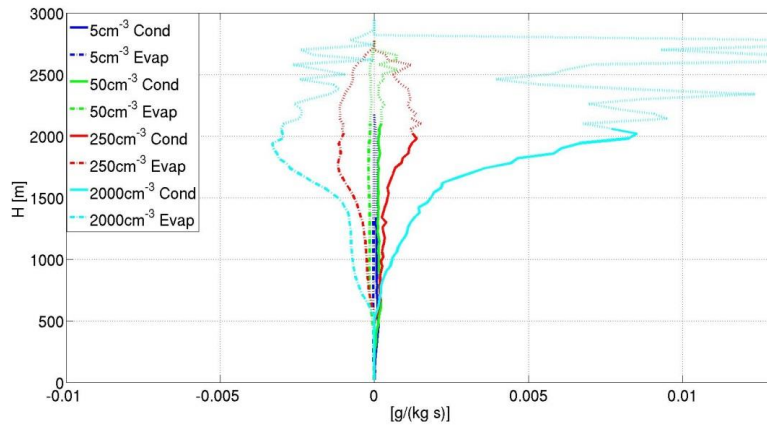


Figure S2. Domain's mean condensation (solid lines) and evaporation (dashed lines) tendencies for four different simulations conducted with different aerosol concentration levels (5 cm^{-3} blue, 50 cm^{-3} green, 250 cm^{-3} red and 2000 cm^{-3} cyan). Note that dotted parts of the curves represent heights in which the total liquid water mass was less than 1% of the maximum total mass (Fig. 4b)."

Second, why is this value so much larger at high altitude than at low altitude, esp for the 2000 cm^{-3} case. Cloud base is somewhere around 500 m (Fig 4), but the mean condensation rate is something like 2 orders of magnitude higher at altitude (2000 to 3000 m). For an adiabatic parcel, the condensation rate generally goes DOWN (albeit not very quickly) with altitude because of the exponential dependence of the saturation mixing ratio on T with the possible exception of the tens of meters near cloud base where there's substantial supersaturation. Also, the difference between the cond and evap tendencies is huge in this area for the 2000 cm^{-3} case. This suggests that LWC should increase greatly at these altitudes (since precip is absent). But Fig. 4 shows that LWC is roughly constant with height in this simulation. I don't think these two are compatible.

Answer: As mentioned above the values calculated in the previous version of Fig. 2 are for the cloudy voxels only. In this case the values of the condensation and evaporation rates increase with height because of the changes in cloud fraction as a function of height (see Fig. R4 below). Naturally, the condensation values were

calculated only for the supersaturated fraction of the domain while the evaporation values are only for the subsaturated fraction.

At the higher end of the vertical cloud extension ($H > 2000\text{m}$) the cloud fraction is extremely low ($< 1\%$) and the subset of supersaturated voxels is smaller. Only the parcels with the strongest vertical velocity and which are closest to adiabatic conditions (high LWC) still have supersaturation at those heights. In those extreme cases the condensation rate can be relatively high. The mean condensation rate for this small fraction of the domain (even if it has large values) is translated into small total condensed mass when looking on the entire domain and integrating over the time (see the new Fig. 2 above). Moreover, the subsaturated fraction of the domain at these heights is larger than the supersaturated fraction and therefore the net condensation-evaporation rate in the polluted simulations is negative.

Following these comments, we added to Fig. 4 in the main text a panel that presents the vertical profile of the total liquid water mass in the domain (Fig. 4b, see below). Figure 4a in the main text presents the mean LWC only for the cloudy voxels while Fig. 4b presents the total water mass per height. Examining both of them together demonstrates that despite the increase in the mean water loading in the upper parts of the clouds with aerosol loading, the total water mass decreases at those layers. Moreover, in order to highlight that the higher parts of the profiles contain small fraction of cloudy voxels, we have marked the heights in which the total mass is less than 1% of the maximum mass (based on Fig. 4b). This was done both in Fig. 4a in the main text and in Figs S1 and S2 in the SI.

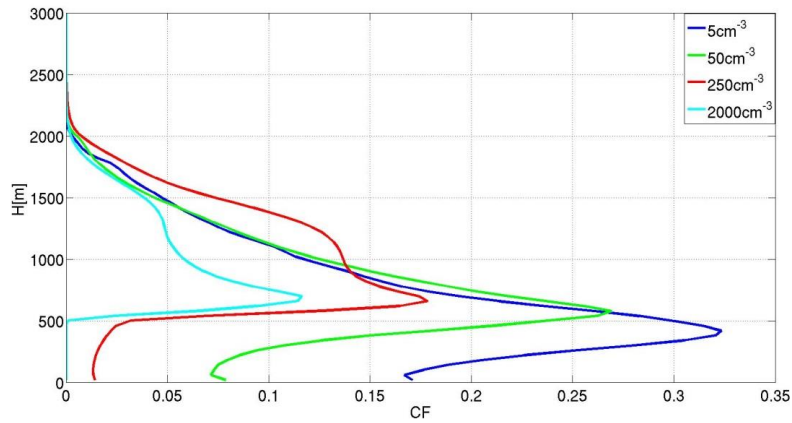


Figure R4. Vertical profiles of the mean (over time and domain) cloud fraction (CF) per height for four simulations (with aerosol loading levels of 5 cm^{-3} – blue, 50 cm^{-3} – green, 250 cm^{-3} – red, and 2000 cm^{-3} – cyan).

The new Fig. 4 in the main text:

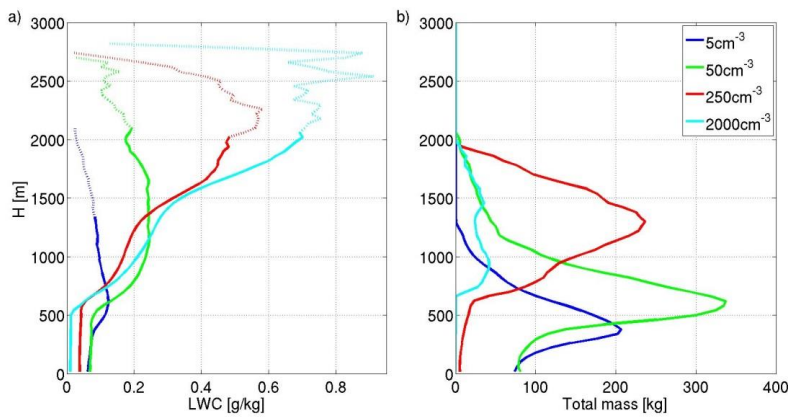


Figure 4. a) Mean liquid water content (LWC) vertical profiles. b) Vertical profiles of the mean (over time) total liquid water mass per height for four different simulations (5 cm^{-3} blue, 50 cm^{-3} green, 250 cm^{-3} red and 2000 cm^{-3} cyan). The mean profiles are calculated for the last 14 hours out of the 16 hours of simulation. Note that dotted parts of the curves in a) represents heights in which the total liquid water mass was less than 1% of the maximum total mass (Fig 4b).

To prevent this confusion, we have changed Fig. 2 to present the total condensed and evaporated mass (and not the mean rates per cloudy voxels). Now, some of the signal is reduced due to the reduction in cloud fraction with aerosol loading.

Lastly, the 1 to 2 orders of magnitude difference between aerosol cases seems wrong. There can be differences (see again Lee et al. 2012) but I don't think they can be that big. By my reasoning, something is very wrong with this plot.

Answer: This brings us back to the answer related to what is presented in the plots. As explained above we do not want to show only the net effect but instead part of this paper's message is that aerosols increase the rates in both directions. Increasing the aerosol concentration increases both condensation and evaporation. Sometimes the net effect can be almost balanced (or be relatively small) not showing this enhancement that in our opinion is responsible to an important part of the aerosol effect. When examining the aerosol effect on the net condensation and evaporation tendencies for the entire domain and the entire time it includes competing effects that reduce the total signal. Specifically, increasing aerosol loading increases both the condensation and evaporation rates and decreases the mean cloud fraction. As explained above, following the editor's comments we have decided to present vertical profiles of the total condensed and evaporated mass which shows a factor of 2-3 difference between clean and polluted simulations.

To avoid the same kind of confusion between averages taken on the whole domain vs. those on cloudy voxels, we also added clarification to the revised manuscript regarding Fig. 4:

"We show that both the height and the magnitude of the maximum LWC increase with the aerosol loading. This is due to both rain suppression (Fig. 1F) and an increased V_{COG} (Fig. 3C) with aerosol loading. There is a reduction in the mean LWP (for $>100 \text{ cm}^{-3}$ - Fig. 1B) although there is an increase in the LWC with aerosol loading due to the differences in cloud fraction (Fig. 1C) and in the vertical distribution of the liquid water (Fig. 4b). At the upper part of the clouds ($H > 2000\text{m}$), in the polluted case, the small amount of cloudy pixels have a large mean LWC (and hence a large water

loading effect) but the total amount of liquid water is small (Fig. 4b). Below the clouds' base ($H < \sim 550\text{m}$) the LWC trend is reversed due to the enhancement of rain in the clean runs (Fig. 1F). The increase in LWC with aerosol loading implies a larger water loading negative component in the clouds' buoyancy."

Fig 1: Panel B does not have units of kg/m^2 . Please include some "uncertainty bars" to indicate the time variability in all panels.

Answer: we thank the editor for this comment. The units in panel B were changed to g/m^2 . The error bars in Fig. 1 present the standard errors which are much smaller than the mean values and than the differences between the simulations.

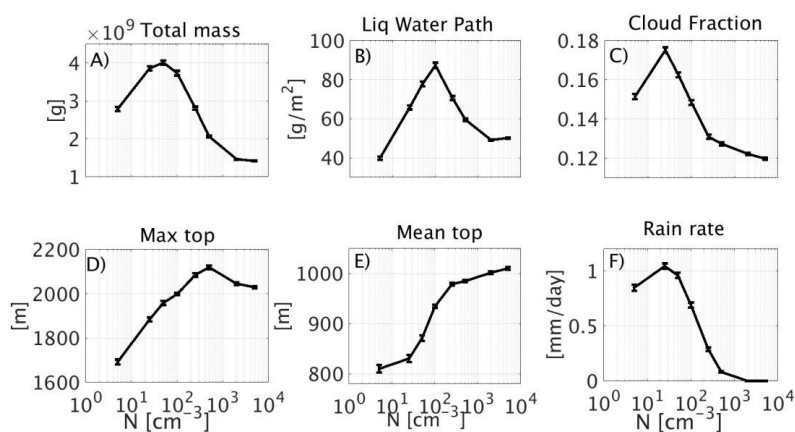


Figure 1. mean properties (over domain and time) of the simulated cloud fields as a function of the aerosol concentration used in the simulation: A) total liquid water mass in the domain, B) cloudy LWP, C) cloud fraction (CF) for columns with $\tau > 0.3$, D) maximum cloud top, E) mean cloud top, and, F) surface rain rate. Each of these mean properties are calculated for the last 14 hours out of the 16 hours of simulation. The error bars present the standard errors. For details about the different properties see the text.

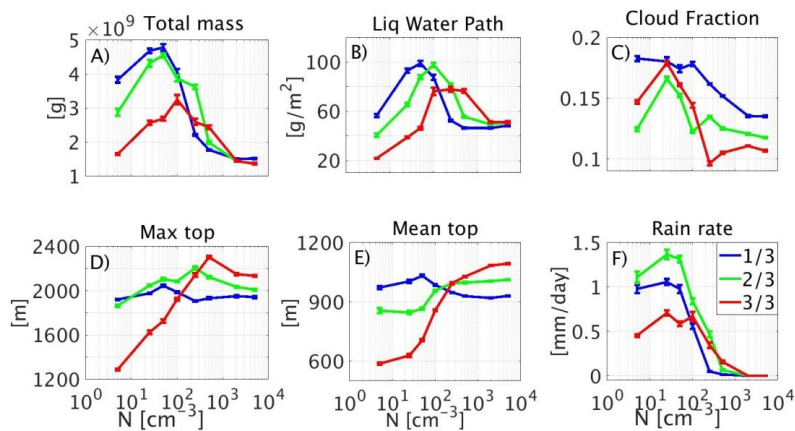


Figure 6. Mean properties (over time and domain) of the simulated cloud fields as a function of the aerosol concentration used in the simulation: A) total liquid water mass in the domain, B) cloudy LWP, C) cloud fraction (CF) for columns with $\tau > 0.3$, D) maximum cloud top, E) mean cloud top, and, F) surface rain rate. Each property is calculated separately for each period of one third of the simulations (blue, green and red for the first, second and third periods, respectively). The error bars present the standard error. For details about the different properties, see the text.

Thanks again for the important comments. We hope that the revised manuscript is clearer.

References

- Grabowski, W. W.: Extracting Microphysical Impacts in Large-Eddy Simulations of Shallow Convection, *Journal of the Atmospheric Sciences*, 71, 4493-4499, 2014.
- Heiblum, R. H., Altaratz, O., Koren, I., Feingold, G., Kostinski, A. B., Khain, A. P., Ovchinnikov, M., Fredj, E., Dagan, G., and Pinto, L.: Characterization of cumulus cloud fields using trajectories in the center of gravity versus water mass phase space: 2. Aerosol effects on warm convective clouds, *Journal of Geophysical Research: Atmospheres*, 2016.
- Jiang, H., Xue, H., Teller, A., Feingold, G., and Levin, Z.: Aerosol effects on the lifetime of shallow cumulus, *Geophysical Research Letters*, 33, 10.1029/2006gl026024, 2006.
- Seifert, A., and Heus, T.: Large-eddy simulation of organized precipitating trade wind cumulus clouds, *Atmos. Chem. Phys*, 13, 5631-5645, 2013.
- Seifert, A., Heus, T., Pincus, R., and Stevens, B.: Large-eddy simulation of the transient and near-equilibrium behavior of precipitating shallow convection, *Journal of Advances in Modeling Earth Systems*, 2015.
- Seigel, R. B.: Shallow Cumulus Mixing and Subcloud Layer Responses to Variations in Aerosol Loading, *Journal of the Atmospheric Sciences*, 2014.
- Xue, H. W., and Feingold, G.: Large-eddy simulations of trade wind cumuli: Investigation of aerosol indirect effects, *Journal of the Atmospheric Sciences*, 63, 1605-1622, 10.1175/jas3706.1, 2006.

Xue, H. W., Feingold, G., and Stevens, B.: Aerosol effects on clouds, precipitation, and the organization of shallow cumulus convection, *Journal of the Atmospheric Sciences*, 65, 392-406, 10.1175/2007jas2428.1, 2008.

Marked-up manuscript version:

Time dependent, non-monotonic response of warm convective cloud fields to changes in aerosol loading

Guy Dagan, Ilan Koren*, Orit Altaratz and Reuven H. Heiblum

Department of Earth and Planetary Sciences, The Weizmann Institute of Science, Rehovot 76100, Israel.

* *Correspondence to:* ilan.koren@weizmann.ac.il

Abstract

Large Eddy Simulations (LES) with bin microphysics are used here to study cloud fields' sensitivity to changes in aerosol properties and the time evolution of this response. Similarly to the known response of a single cloud, we show that the mean field properties change in a non-monotonic trend, with an optimum aerosol concentration for which the field reaches its maximal water mass or rain yield. This trend is a result of competition between processes that encourage cloud development versus those that suppress it. However, another layer of complexity is added when considering clouds' impact on the field's thermodynamic properties and how this is dependent on aerosol loading. Under polluted conditions rain is suppressed and the non-precipitating clouds act to increase atmospheric instability. This results in warming of the lower part of the cloudy layer (in which there is net condensation) and cooling of the upper part (net evaporation). Evaporation at the upper part of the cloudy layer in the polluted simulations raises humidity at these levels and thus amplifies the development of the next generation of clouds (preconditioning effect). On the other hand, under clean conditions, the precipitating clouds drive net warming of the cloudy layer and net cooling of the sub-cloud layer due to rain evaporation. These two effects act to stabilize the atmospheric boundary layer with time (consumption of the instability). Evolution of the field's thermodynamic properties affects the cloud properties in return, as shown by migration of the optimal aerosol concentration toward higher values.

1. Introduction

Despite the extensive research conducted in the last few decades, and the fact that clouds have an important role in the Earth's energy balance (Trenberth et al., 2009) clouds are still considered to be one of the largest source of uncertainty in the study of climate and climate change (Forster et al., 2007; Boucher et al., 2013).

Warm cloud (containing liquid water only) formation depends on the availability of water vapor and aerosols acting as cloud condensation nuclei (CCN). Changes in aerosol concentration modulate the cloud droplet size distribution and total number. Polluted clouds (forming under high aerosol loading) initially have smaller and more numerous droplets, with narrower size distribution compared to clean clouds (Squires, 1958; Squires and Twomey, 1960; Warner and Twomey, 1967; Fitzgerald and Spyers-Duran, 1973).

The initial droplet size distribution affects key cloud processes such as condensation-evaporation, collision-coalescence and sedimentation. The condensation-evaporation process is proportional to the total droplet surface area which increases with the droplet number concentration (for a given total liquid water mass). Under given supersaturation conditions, the condensation in polluted clouds is more efficient ([higher condensation rate or shorter consumption time of the supersaturation](#) - (Pinsky et al., 2013; Seiki and Nakajima, 2014; Koren et al., 2014; Kogan and Martin, 1994; Dagan et al., 2015a). However, under sub-saturation conditions, due to the same reason, it implies higher evaporation efficiency. The evaporation induces downdrafts and stronger vorticity and hence can lead to stronger mixing of the cloud with its environment in polluted conditions (Xue and Feingold, 2006; Jiang et al., 2006; Small et al., 2009).

The initiation of collision-coalescence is delayed in polluted clouds (Gunn and Phillips, 1957; Squires, 1958; Albrecht, 1989). This drives a delay in rain formation and can affect the amount of surface rain (Rosenfeld, 1999, 2000; Cheng et al., 2007; Khain, 2009; Levin and Cotton, 2009; Koren et al., 2012; Hazra et al., 2013a,b; Dagan et al., 2015b).

Aerosol effects on single warm convective clouds were shown to have an optimal value with respect to maximal water mass, cloud depth and rain yield (Dagan et al., 2015a,b), which depends on the environmental conditions. For aerosol concentrations lower than the optimum, the positive relationship between aerosol concentration and cloud development is a result of two main processes: 1) larger latent heat release driven by the increase in the condensation efficiency causing stronger updrafts, and 2) decrease in the effective terminal velocity (η , i.e. mass weighted terminal velocity of the hydrometeors) (Koren et al., 2015) due to initial smaller droplets and the delay in the collision-coalescence process. The smaller droplets have higher mobility (the water mass moves up better with surrounding updraft), reaching higher in the atmosphere and prolonging the cloud growth.

For aerosol concentration values above the optimum, the suppressing aerosol effects take over, namely: 1) stronger mixing of the cloud with its environment driven by the increased evaporation efficiency (Small et al., 2009), and 2) increased water loading effect due to the rain suppression.

Understanding of the overall aerosol effect is even more complex when considering processes on the cloud field scale. Clouds affect the surrounding thermodynamic conditions by changing the humidity and temperature profiles (Lee et al., 2014; Seifert et al., 2015; Stevens and Feingold, 2009; Saleeby et al., 2015). In addition, clouds affect the solar and longwave radiation budgets in the field. Over land the radiation effects change the surface temperature and therefore can significantly affect heat and moist fluxes, and as a result the cloud properties (Koren et al., 2004, 2008; Feingold et al., 2005).

The invigoration mechanism, which refers to deeper and larger clouds with larger mass that develop under polluted conditions was studied mainly in deep convective clouds (Andreae et al., 2004; Koren et al., 2005; Rosenfeld et al., 2008; Tao et al., 2012; Fan et al., 2013; Hazra et al., 2013a; Altaratz et al., 2014). Our focus here is on warm cloud fields for which previous observational studies reported on invigoration effect or a non-monotonic response of the clouds to an increase in aerosol loading. For example, Kaufman et al., (2005) found an increase in cloud fraction (CF) of warm cloud fields with increasing aerosol loading over the tropical Atlantic Ocean. Yuan et al. (2011) reported that an increase in volcanic aerosols near Hawaii led to increased

trade cumulus CF and clouds top height. Dey et al. (2011) have shown that an increase in aerosol optical depth (AOD) from clean to slightly polluted resulted in an increase in CF in warm clouds over the Indian Ocean. Additional increase in the AOD resulted in a decrease of CF, explained by the semi direct effect of absorbing aerosols. Costantino and Bréon (2013) reported higher CF over the south-eastern Atlantic under high aerosol loading conditions. From convective stability considerations deeper clouds tend to have larger area (larger CF). It was shown that warm convective cloud's area correlates positively with cloud's depth (Benner and Curry, 1998; Koren et al., 2008).

Koren et al. (2014) have shown that warm convective clouds over the Southern Oceans can be considered as aerosol limited up to moderate aerosol loading conditions. As the AOD increases, the clouds were shown to be deeper and larger, and to produce stronger rain rates. A reversal in trend of liquid water path (LWP) as a function of increasing AOD was reported using observations of warm convective clouds under large range of meteorological conditions (Savane et al., 2015). Li et al. (2011) studied warm clouds over the southern great plains of the United States and reported no aerosol effect on clouds' top height.

On the other hand, numerical studies of the aerosol's effect on warm cumulus cloud fields show either no effect or cloud suppression (meaning shallower and smaller clouds under higher aerosol loading conditions). Jiang and Feingold (2006) found that the LWP, CF, and cloud depth of warm shallow convective clouds are insensitive to an increase in aerosol loading. However, they did demonstrate rain suppression by aerosols. Xue et al. (2008) showed smaller clouds and suppression of precipitation in increased aerosol loading environment. Jiang et al. (2010) found a non-monotonic change in the derivative of the surface rain rate with aerosol loading (susceptibility) for higher maximal LWP clouds, but a monotonic decrease in the total precipitation with aerosol loading. Seigel (2014) showed that the clouds' size decreases with aerosol loading due to enhanced entrainment at clouds' margins.

Some previous studies have demonstrated clouds alteration of their environment (Zhao and Austin, 2005; Heus and Jonker, 2008; Malkus, 1954; Lee et al., 2014; Zuidema et al., 2012; Roesner et al., 1990). One example of such effect is the

"preconditioning" or "cloud deepening" effect (Nitta and Esbensen, 1974; Roesner et al., 1990; Stevens, 2007; Stevens and Seifert, 2008), where clouds cool and moisten the upper cloudy and inversion layers and by that encourage the development of the next generation of clouds that encounter improved environmental conditions. This effect is influenced by the clouds' microphysical properties (Stevens and Feingold, 2009; Saleeby et al., 2015). The role of warm convective clouds in moistening of the free troposphere was studied intensively using both observations and cloud field numerical models (Brown and Zhang, 1997; Johnson et al., 1999; Takemi et al., 2004; Kuang and Bretherton, 2006; Holloway and Neelin, 2009; Waite and Khouider, 2010).

Albrecht (1993) used a theoretical single column model to study the effect of precipitation on the thermodynamic structure of trade wind boundary layer and found that even low rain rates can dramatically affect the profiles. Under precipitating conditions, the cloud layer is warmer, drier, and more stable than under non-precipitation conditions. He also showed that under non-precipitating conditions the inversion height is greater than under precipitating conditions, due to the larger amount of liquid water evaporated at those elevations.

Another way clouds effect their environment is by evaporation of rain below the cloud base which induces cooling of the sub-cloudy layer (Zuidema et al., 2012; Heiblum et al., 2016a). Lee et al. (2014) demonstrated the aerosol effects on the field's CAPE (as distributed above cloud base or below it). The organization of the field is influenced by cloud processes as well. Enhanced evaporative cooling in the sub-cloud layer, for example, can produce cold pools which enhance the generation of clouds only at their boundaries, and hence change the organization of the field (Seigel, 2014; Seifert and Heus, 2013; Heiblum et al., 2016a).

A recent paper (Dagan et al., 2016) showed that polluted clouds act to increase the thermodynamic instability with time, while clean clouds consume the atmospheric instability. The trend of the pollution driven increase in the instability is halted once the clouds are thick enough to develop significant precipitation. Indeed, studies of long simulation times (>30 hr), showed that the initial differences between clean and polluted cases are reduced by negative feedbacks of the clouds on the thermodynamic conditions (Lee et al., 2012; Seifert et al., 2015).

In this work we explore the coupled microphysical-dynamic system of warm marine cloud fields [using a bin-microphysics scheme under a large range of aerosol concentrations](#). [We study the aerosol-cloud-environmental thermodynamic system by examining how changes in aerosol concentrations affect clouds properties, the related modifications of the thermodynamic conditions over time which as well drive feedbacks on the clouds' properties evolution.](#)

2. Methodology

The SAM (System for Atmospheric Modeling), non-hydrostatic, anelastic LES model version 6.10.3 (Khairoutdinov and Randall, 2003) was used to simulate the well-studied trade cumulus case of BOMEX (Holland and Rasmusson, 1973; Siebesma et al., 2003). The BOMEX case is an idealized trade-cumulus cloud field that is based on observations made near Barbados during June 1969. This case was initialized using the setup specified in Siebesma et al. (2003). The setup includes surface fluxes and large scale forcing (see details in Heiblum et al., 2016b). The horizontal resolution was set to 100 m while the vertical resolution was set to 40 m. The domain size was 12.8 x 12.8 x 4.0 km³ and the time step was 1 sec. Due to computational limitations, we had to restrict the domain size to a scale that has a limited capability for capturing large scale organization (Seifert and Heus, 2013). The model ran for sixteen hours and the statistical analysis included all but the first two hours (total of 14 hours). [After 2 h of simulations the initial increase in the total liquid water mass in the domain desisted and the differences between the simulations \(differ by the aerosol loading\) became significant. Therefore 2h is determined as spin-up time \(similar to the spin-up time in Xue and Feingold, 2006\).](#)

A bin microphysical scheme (Khain and Pokrovsky, 2004) was used. The scheme solves warm microphysical processes, including droplet nucleation, diffusional growth, collision coalescence, sedimentation and breakup.

[In order to focus on the aerosol effect on the thermodynamic properties of the field, the radiative effects \(as included in the large scale forcing - see details in Dagan et al., 2016\) were prescribed in all simulations. The aerosol distribution adopts a marine size distribution \(see details in Jaenicke 1988 and Altaratz et al., 2008\). Eight different simulations were conducted simulating a wide range of aerosol loading conditions from extremely pristine to polluted \(total concentration of: 5, 25, 50, 100, 250, 500, 2000 and 5000 cm⁻³ near ground level, Dagan et al., 2015a\). To reduce the results](#)

sensitivity to the [shape of the](#) aerosol size distribution ~~shape~~ and to focus on the aerosol number concentration effect, the different aerosol concentrations are calculated by multiplication of all bins ~~in the smallest concentration size distribution~~ by a constant factor and maintaining a similar shape of the size distribution. The aerosol is assumed to be composed of ammonium-sulfate and [initialized with](#) ~~maintains~~ constant mixing ratio with height. A prognostic equation is solved for the aerosol mass, including regeneration upon evaporation and removal by surface rain. Regeneration upon evaporation of cloud drops was shown to be a very important source of aerosols, especially in polluted conditions (Yin et al., 2005). The aerosol serves as potential cloud condensation nuclei (CCN) and it is activated based on the Kohler theory ([the scheme is described in](#) Khain et al., 2000). The aerosol (water drop) size distribution is calculated between 5 nm to 2 μm (2 μm -3.2 mm). For both aerosol and drops, successive bins represent doubling of the mass.

The effects of changes in aerosol concentration on the drop concentration and its mean size, for the different simulations can be found in Fig. S1 in the supporting information (SI).

3. Results and discussion

3.1 Mean cloud field properties under different aerosol loading conditions

[The aerosol effects on the mean field properties during the entire run are examined first following by a more detailed examination of the time evolution in the next section.](#) Figure 1 presents mean values of key properties of cloud fields as a function of the aerosol loading for the entire (14 h) simulation time.

The total water mass (calculated as mean over time in each domain) as a function of aerosol concentration shows a clear reversal in the trend (Fig. 1A). For the given environmental conditions simulated here, it increases when increasing aerosol loading from 5 to 50 cm^{-3} . Additional increase in the aerosol loading results in a decrease in the total water mass in the domain.

The LWP (Liquid Water Path - Fig. 1B) calculated as a mean over time over all cloudy columns in each domain, which is strongly correlated with the total water mass, also shows the same non-monotonic general trend. The maximum in the curve of cloudy LWP is at slightly higher aerosol concentration compared to the total mass (100 cm^{-3}). This difference can be explained by the link to the cloud fraction (CF – calculated as the area covered by clouds with optical path $\tau > 0.3$ Fig. 1C) that

decreases above aerosol loading of 25 cm^{-3} . And so, for the more polluted simulations the mass is distributed on smaller horizontal cloud areas as shown in previous studies (Seigel, 2014).

There is also a significant difference in the way the water mass is distributed along the atmospheric column in the different simulations. The maximum cloud top height (Fig. 1D), calculated as a mean over time of the altitude of the highest grid box in the domain that contains liquid water content ($\text{LWC} > 0.01 \text{ g/kg}$) increases significantly when increasing aerosol loading up to 500 cm^{-3} (increase from 1692 m to 2120 m when increasing aerosol loading from 5 to 500 cm^{-3}). Additional increase in the aerosol loading results in a minor decrease in the maximum cloud top height (down to 2030 m for aerosol loading of 5000 cm^{-3}). The minor decrease seen for this range of aerosol concentration (compared with the larger decrease in the mean LWP for example) can be explained by the location of the maximal cloud top height above the cloud core, which is affected mainly by the invigoration processes (enhanced condensation and latent heat release) and less by margin oriented processes (enhanced entrainment and evaporation) that significantly impact the total cloud mass (Dagan et al., 2015a). Another reason is the cloud deepening effect under polluted conditions (Stevens, 2007; Seifert et al., 2015) that will be described later. As for the mean cloud top height calculated as a mean of all cloudy columns along the whole run (Fig. 1E), the trend shows a monotonic increase with aerosol loading. The trend is approaching a saturation level for high aerosol concentration values. The mean cloud top value over the simulation is 810 and 1010 m for the simulations with aerosol loading of 5 to 5000 cm^{-3} , respectively.

[Presenting together the mean over time of the maximum and the mean cloud top height captures, in a compact, yet informative, way the response of the cloud top height distribution to changes in aerosol loading and reduces the sensitivity to outliers. Moreover, by averaging over time the significance of the outliers is decreased as well.](#)

The trend in the domain's average rain rate, as a function of the aerosol loading (Fig. 1F) shows a peak at relatively low aerosol loading (similar to optimal value of the CF) of 25 cm^{-3} .

Fig. 2 presents the vertical profiles of the total condensed and evaporated mass during the simulations ~~mean vertical profiles of the condensation evaporation tendencies~~, for four different simulations. We note that as the aerosol loading increases, both the the mean condensated condensed and evaporated massion rates increased (this is due to the increase in the diffusion rates – see Fig. S2, SI, and despite the decrease in cloud fraction – see Fig. 1C, Dagan et al., 2015a; Koren et al., 2014; Pinsky et al., 2013; Seiki and Nakajima, 2014). Below cloud base (located around 550 m) the clean simulations have small rain evaporation values which is absent in the polluted simulations.

Effective terminal velocity (η) is defined as the mass weighted average terminal velocity of all the hydrometeors within a given volume of air (Koren et al., 2015). By definition, η measures the terminal velocity of the water mass's center of gravity (COG), i.e. the COG's movement with respect to the surrounding air's vertical velocity (W). Small absolute values $|\eta|$ imply that the droplets COG will move better with the surrounding air, i.e. the droplets will have better mobility (Koren et al., 2015). The sum $V_{COG} = W + \eta$ (η always negative) reflects the water mass COG vertical velocity relative to the surface. Positive V_{COG} implies a rise of the COG, and negative value means falling.

The mean updraft (in both space and time, weighted by the liquid water mass in each grid box to be consistent with the COG point of view - Fig. 3A) increases with the increase in aerosol loading, in agreement with previous studies (Saleeby et al., 2015; Seigel, 2014). This indicates an increase in the latent heat contribution to the cloud buoyancy, driven by increase in the condensation efficiency (Dagan et al., 2015a,b; Koren et al., 2014; Pinsky et al., 2013; Seiki and Nakajima, 2014) (Fig. 2 and Fig S2, SI). At the same time, $|\eta|$ decreases as the aerosol concentration increases (Fig. 3B) indicating better mobility of the smaller droplets, allowing them to move more easily with the air's updrafts. The outcome of these two effects is an increased V_{COG} for higher aerosol concentration (Fig. 3C) indicating that the polluted clouds' liquid water is pushed higher in the atmosphere (Koren et al., 2015) as shown by higher COG (Fig. 3D).

The mean COG height of the water mass (Grabowski et al., 2006; Koren et al., 2009) (Fig. 3D), increases with the aerosol loading up to a relatively high concentration (500 cm^{-3}). Note that while the trend in the system's characteristic velocities (η and W) is monotonic increase, the COG has an optimal aerosol concentration for which it reaches its maximum height (500 cm^{-3}). For aerosol concentrations above 500 cm^{-3} a minor decrease is shown. As described above, the COG height increase with aerosol loading, between extremely clean and polluted conditions, can be explained by increased V_{COG} , which is a product of both lower $|\eta|$ and increased updraft in the cloud scale, and larger thermodynamic instability induced by the polluted clouds in the field scale as will be shown in the next section (Dagan et al., 2016; Heiblum et al., 2016a). The reduction of the mean COG height in the most polluted simulations is caused by cloud suppressing processes including an enhanced entrainment (see the enhanced evaporation efficiency with aerosol loading – Fig. 2 and Fig. S2, SI) and larger water loading (Dagan et al., 2015a - shown also in Fig. 4a below).

The trend in COG height can be also viewed (in more detail) in Fig. 4a that presents profiles of mean LWC [for cloudy voxels only](#).

We show that both the height and the magnitude of the maximum LWC increase with the aerosol loading. This is due to both rain suppression (Fig. 1F) and an increased V_{COG} (Fig. 3C) with aerosol loading. There is a reduction in the mean LWP (for $>100 \text{ cm}^{-3}$ - Fig. 1B) although there is an increase in the LWC with aerosol loading due to the differences in cloud fraction (Fig. 1C) [and in the vertical distribution of the liquid water \(Fig. 4b\)](#). [At the upper part of the clouds \(\$H > 2000\text{m}\$ \), in the polluted case, a small amount of cloudy pixels have a large mean LWC \(and hence a large water loading effect\) but the total amount of liquid water is small \(Fig. 4b\)](#). Below the clouds' base ($H < \sim 550\text{m}$) the LWC trend is reversed due to the enhancement of rain in the clean runs (Fig. 1F). The increase in LWC with aerosol loading implies a larger water loading negative component in the clouds' buoyancy.

All the evidence presented in Figs. 2-4 explains the non-monotonic trends of the clouds properties response to changes in aerosol loading (Fig. 1). For clean conditions (below the optimal aerosol concentration value), an increase in aerosol loading would enhance the cloud development (larger mass, LWP, cloud top, CF, rain rate) because

of two main factors: 1) an increase in the condensation efficiency (due to the larger total droplet surface area for condensation and longer time- Fig. 2 [and Fig S2, SI](#)), and 2) smaller effective terminal velocity (η) values, that per given updraft allow the cloud's hydrometeors to be pushed higher in the atmosphere (Koren et al., 2015) (Fig. 3B).

The higher condensation efficiency in polluted clouds (Fig. 2) results in a larger latent heat release that enhances the updraft (Fig. 3A) and cloud development. The increased V_{COG} reflects the two cloud enhancing processes (decrease in $|\eta|$ and larger mean updraft). We note that the increase in the mean updraft values with aerosol loading is seen despite the negative effect of water loading (see Fig. 4a). For aerosol concentrations above the optimum, cloud development is suppressed by the increase in evaporation efficiency (Fig. 2) and hence stronger mixing of the cloud with its environment (i.e. Small et al., 2009), and larger water loading due to rain suppression (Dagan et al., 2015a, Fig. 4a).

3.2 The time evolution of the mean cloud field properties under different aerosol loading conditions

All the aerosol effects that were discussed up to this point (condensation-evaporation efficiencies, η and water loading) are applicable both on the single cloud scale as well as on the cloud field scale. However, on the cloud field scale, another aspect needs to be considered, namely the time evolution of the effect of clouds on the field's thermodynamic conditions (which was the focus of a recent study by Dagan et al., 2016).

Figure 5 presents the changes (final value minus initial one) in the temperature (T) and water vapor content (q_v) vertical profiles as a function of aerosol concentration used in the simulation. The initial profiles were identical in all simulations. Figure S3 (in the SI) presents the full temporal evolution of those parameters. In low aerosol concentration runs (100 cm^{-3} and below) the sub-cloud layer becomes cooler and wetter with time and the cloudy layer warmer and drier. Meanwhile, under higher

aerosol concentrations conditions (250 cm^{-3} and above) the sub-cloud layer becomes warmer and drier while the cloudy and inversion layers become colder and wetter. This trend is driven by the condensation-evaporation tendencies along the vertical profile (see Fig. 2, Dagan et al., 2016). Under low aerosol concentration conditions, water condenses at the cloudy layer and is advected downward to the sub-cloud layer where it partially evaporates. Under polluted conditions, on the other hand, the condensed water from the lower part of the cloudy layer is advected up to the upper cloudy and inversion layers (driven by larger V_{COG} - Fig. 3) and evaporates there (Dagan et al., 2016).

Such trends in the environmental thermodynamic conditions are likely to affect the forming clouds. In Fig. 6 the time evolution of some of the key cloud field properties are considered (the same properties that were shown in Fig. 1). The blue, green and red curves represent the mean values over the first, second and third periods of the simulations, respectively (each one covers 4 hours and 40 min). Table 1 presents change (in percentage) in the mean values of key variables between the third period of the 8 simulations (during the 11:20-16:00 hours of simulation, red curves in Fig. 6) and the first period (02:00-06:40 hours of simulation, blue curves in Fig. 6).

Examination of the evolution in the mean total water mass along the simulations (Fig. 6A blue, green and red curves) presents a different trend between the clean and the polluted simulations. In the clean simulations ($5\text{-}100 \text{ cm}^{-3}$) the total water mass decreases significantly with time (a decrease of 57, 45, 44, 20% in the total mass for the cases of 5, 25, 50 and 100 cm^{-3} respectively – see table 1). On the other hand, in the more polluted simulations, (with aerosol loading of 250 and 500 cm^{-3}) there is an increase in the total water mass with time (of 17 and 37% between the first and the last third periods of the simulations, respectively). Under extreme polluted conditions of 2000 and 5000 cm^{-3} , the total water mass in the domain is small and there is little change with time. These changes in time push the optimum aerosol concentration to higher values along the simulation time. This trend is also shown for the optimum aerosol concentration with regard to the mean cloudy LWP (Fig. 6B), max top (Fig. 6D) and mean top (Fig. 6E).

Trends in the mean rain rate show that in the cleanest simulations (5, 25 and 50 cm^{-3}) it decreases with time (Fig. 1H, 53.3, 32.9 and 40.1%, respectively). In the regime of medium to fairly high aerosol loading (100, 250 and 500 cm^{-3}) the rain rate increases (19.6, 598.1 and 841.5%, respectively). And in the most polluted simulations (2000 and 5000 cm^{-3}) the surface rain is negligible throughout the simulation time. These trends are explained below.

The time evolution of the thermodynamic conditions (Fig. 5) shows a reduction (enhancement) in the thermodynamic instability with time in the clean (polluted) simulations. Figure 6 and table 1 indicate that under clean conditions the decrease in the thermodynamic instability with time leads to a decrease in the mean cloud field properties such as total mass, cloud top height and rain rate. Under polluted conditions the trends are opposite and the mean cloud field properties increase with time due to the increase in thermodynamic instability (Dagan et al., 2016) and due to the cloud deepening (Stevens and Seifert, 2008; Stevens, 2007; Seifert et al., 2015). These differences between the clean and polluted simulations drive changes in the optimum aerosol concentration with time. For example, for the LWP (Fig. 1B) the optimum aerosol concentration is 50, 100 and 250 cm^{-3} for the first, second and third parts of the simulation, respectively.

Summary

Cloud processes can be divided in a simplistic manner into two characteristic scales – the cloud scale and the field scale. Here using LES model with bin microphysical scheme we studied the outcome of the two scales' processes acting together. We first presented domain averaged properties over the whole simulation time (section 3.1) to indicate the general aerosol effects in a first order manner and then we followed the time evolution of the effects (section 3.2).

A non-monotonic aerosol effect was reported recently for a single cloud scale (Dagan et al., 2015a,b). Here we show that these trends “survived” the domain and time averaging. We argue that the enhanced development branch trend is driven by two main processes of enhanced condensation and reduced effective terminal velocity (which improves the droplets mobility). These processes are mainly related to the core

of the clouds and to the early stages of clouds development. We show that the cloud's systems characteristic velocities can capture these effects. The effective terminal velocity (η) inversely measures the mobility. Smaller droplets with smaller variance will have smaller η and therefore will be pushed higher in a given updraft, whereas larger droplets with larger η will deviate downward faster from the surrounding air. Increase in condensation efficiency drives more latent heat release that enhances the cloud updraft. We showed that V_{COG} is a product of the two velocities.

The descending branch in which increase of aerosol loading suppresses cloud development is governed by increase in the evaporation efficiency on the subsaturated parts of the clouds and by increase in water loading.

Since clouds change the atmospheric thermodynamic conditions in which they form, different initial clouds would cause different impact on the environment. Therefore, cloud field is a continuously evolving system for which aerosol properties determine an important part of the temporal trends. Figure 5 shows striking differences between the evolution of the thermodynamic profiles in clean and polluted cases. For the polluted clouds (mostly non-precipitating), the upper cloudy layer turns wetter and cooler due to enhanced evaporation and the sub-cloudy layer becomes warmer and drier, which altogether act to increase the instability. On the other hand, clean precipitating clouds consume the initial instability with time by warming the cloudy layer (due to latent heat release) and cooling the sub-cloud layer by evaporation of rain.

The polluted cloud feedbacks on the thermodynamic conditions act to deepen the clouds. Since clouds that form in a more unstable environment are expected to be aerosol limited up to higher aerosol concentrations (Koren et al., 2014; Dagan et al., 2015a), an increase in the domains instability for the polluted cases drives an increase in the optimal aerosol concentration with time.

We note that such an increase in the instability cannot last forever. A deepened cloud will eventually produce larger precipitation rates that may weaken the overall effect on the field (Stevens and Feingold, 2009; Seifert et al., 2015). These results pose an interesting question on the dynamical state of cloud fields in nature. Do the cloud fields 'manage' to reach a "near-equilibrium" state (Seifert et al., 2015), for which the deepening effect balances the aerosol effect fast enough that the effects are buffered most of the time (Stevens and Feingold, 2009). Or maybe, the characteristic lifetime

of a trade cumulus cloud field is shorter than the time it takes to significantly balance the aerosol effects. In this case the cloud fields could be regarded as ‘transient’ and therefore, as shown here, aerosol might have a strong effect on the clouds, both through affecting the microphysics, initiating many feedbacks in the cloud scale, and by affecting the field thermodynamic evolution over time.

Acknowledgements

This research has been supported by the Minerva foundation with funding from the Federal German Ministry of Education and Research.

References

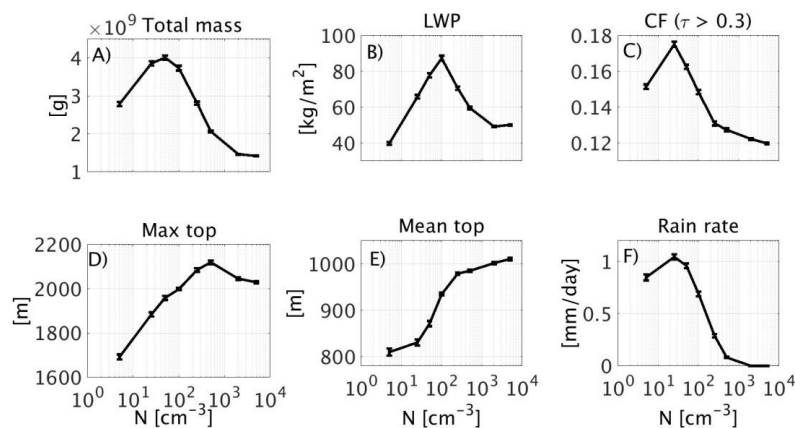
- Albrecht, B. A.: Aerosols, cloud microphysics, and fractional cloudiness, *Science* (New York, NY), 245, 1227, 1989.
- Albrecht, B. A.: Effects of precipitation on the thermodynamic structure of the trade wind boundary layer, *Journal of Geophysical Research: Atmospheres* (1984–2012), 98, 7327-7337, 1993.
- Altaratz, O., Koren, I., Reisin, T., Kostinski, A., Feingold, G., Levin, Z., and Yin, Y.: Aerosols' influence on the interplay between condensation, evaporation and rain in warm cumulus cloud, *Atmospheric Chemistry and Physics*, 8, 15-24, 2008.
- Altaratz, O., Koren, I., Remer, L., and Hirsch, E.: Review: Cloud invigoration by aerosols—Coupling between microphysics and dynamics, *Atmospheric Research*, 140, 38-60, 2014.
- Andreae, M. O., Rosenfeld, D., Artaxo, P., Costa, A. A., Frank, G. P., Longo, K. M., and Silva-Dias, M. A. F.: Smoking rain clouds over the Amazon, *Science*, 303, 1337-1342, 10.1126/science.1092779, 2004.
- Benner, T. C., and J. A. Curry: Characteristics of small tropical cumulus clouds and their impact on the environment, *J. Geophys. Res.*, 103(D22), 28753–28767, doi:[10.1029/98JD02579](https://doi.org/10.1029/98JD02579), 1998.
- Boucher, O., Randall, D., Artaxo, P., Bretherton, C., Feingold, G., Forster, P., Kerminen, V., Kondo, Y., Liao, H., and Lohmann, U.: Clouds and aerosols, *Climate Change*, 571-657, 2013.
- Brown, R. G., and Zhang, C.: Variability of midtropospheric moisture and its effect on cloud-top height distribution during TOGA COARE*, *Journal of the atmospheric sciences*, 54, 2760-2774, 1997.
- Cheng, C.-T., W.-C. Wang, and J.-P. Chen: A modelling study of aerosol impacts on cloud microphysics and radiative properties, *Quarterly Journal of the Royal Meteorological Society*, 133(623), 283-297, 2007.
- Costantino, L., and Bréon, F.-M.: Aerosol indirect effect on warm clouds over South-East Atlantic, from co-located MODIS and CALIPSO observations, *Atmospheric Chemistry and Physics*, 13, 69-88, 2013.
- Dagan, G., Koren, I., and Altaratz, O.: Competition between core and periphery-based processes in warm convective clouds—from invigoration to suppression, *Atmospheric Chemistry and Physics*, 15, 2749-2760, 2015a.
- Dagan, G., Koren, I., and Altaratz, O.: Aerosol effects on the timing of warm rain processes, *Geophysical Research Letters*, 42, 4590-4598, 10.1002/2015GL063839, 2015b.

- Dagan, G., Koren, I., Altaratz, O., and Heiblum, R. H.: Aerosol effect on the evolution of the thermodynamic properties of warm convective cloud fields, *Scientific Reports*, in press, 2016.
- Dey, S., Di Girolamo, L., Zhao, G., Jones, A. L., and McFarquhar, G. M.: Satellite-observed relationships between aerosol and trade-wind cumulus cloud properties over the Indian Ocean, *Geophysical Research Letters*, 38, 2011.
- Fan, J., Leung, L. R., Rosenfeld, D., Chen, Q., Li, Z., Zhang, J., and Yan, H.: Microphysical effects determine macrophysical response for aerosol impacts on deep convective clouds, *Proceedings of the National Academy of Sciences*, 110, E4581-E4590, 2013.
- Feingold, G., Jiang, H. L., and Harrington, J. Y.: On smoke suppression of clouds in Amazonia, *Geophysical Research Letters*, 32, 10.1029/2004gl021369, 2005.
- Fitzgerald, J., and Spyers-Duran, P.: Changes in cloud nucleus concentration and cloud droplet size distribution associated with pollution from St. Louis, *Journal of Applied Meteorology*, 12, 511-516, 1973.
- Forster, P., Ramaswamy, V., Artaxo, P., Bernsten, T., Betts, R., Fahey, D. W., Haywood, J., Lean, J., Lowe, D. C., Myhre, G., Nganga, J., Prinn, R., Raga, G., Schulz, M., and Dorland, R. V.: Changes in Atmospheric Constituents and in Radiative Forcing., in: *Climate Change 2007: The Physical Science Basis. Contribution of Working Group I to the Fourth Assessment Report of the Intergovernmental Panel on Climate Change*, edited by: Solomon, S., D. Qin, M. Manning, Z. Chen, M. Marquis, K.B. Averyt, M.Tignor and H.L. Miller Cambridge University Press, Cambridge, United Kingdom and New York, NY, USA., 2007.
- Grabowski, W., Bechtold, P., Cheng, A., Forbes, R., Halliwell, C., Khairoutdinov, M., Lang, S., Nasuno, T., Petch, J., and Tao, W. K.: Daytime convective development over land: A model intercomparison based on LBA observations, *Quarterly Journal of the Royal Meteorological Society*, 132, 317-344, 2006.
- Gunn, R., and Phillips, B.: An experimental investigation of the effect of air pollution on the initiation of rain, *Journal of Meteorology*, 14, 272-280, 1957.
- Hazra, A., B. Goswami, and J.-P. Chen: Role of interactions between aerosol radiative effect, dynamics, and cloud microphysics on transitions of monsoon intraseasonal oscillations, *Journal of the Atmospheric Sciences*, 70(7), 2073-2087, 2013a.
- Hazra, A., P. Mukhopadhyay, S. Taraphdar, J. P. Chen, and W. R. Cotton: Impact of aerosols on tropical cyclones: An investigation using convection-permitting model simulation, *Journal of Geophysical Research: Atmospheres*, 118(13), 7157-7168, 2013b.
- Heiblum, R. H., Altaratz, O., Koren, I., Feingold, G., Kostinski, A. B., Khain, A. P., Ovchinnikov, M., Fredj, E., Dagan, G., and Pinto, L.: Characterization of cumulus cloud fields using trajectories in the center-of-gravity vs. water mass phase space. Part II: Aerosol effects on warm convective clouds, *Journal of Geophysical Research: Atmospheres*, 2016a.
- Heiblum, R. H., Altaratz, O., Koren, I., Feingold, G., Kostinski, A. B., Khain, A. P., Ovchinnikov, M., Fredj, E., Dagan, G., and Pinto, L.: Characterization of cumulus cloud fields using trajectories in the center of gravity versus water mass phase space: 1. Cloud tracking and phase space description, *Journal of Geophysical Research: Atmospheres*, 2016b.
- Heus, T., and Jonker, H. J.: Subsiding shells around shallow cumulus clouds, *Journal of the Atmospheric Sciences*, 65, 1003-1018, 2008.
- Holland, J. Z., and Rasmusson, E. M.: Measurements of the atmospheric mass, energy, and momentum budgets over a 500-kilometer square of tropical ocean, *Monthly Weather Review*, 101, 44-55, 1973.
- Holloway, C. E., and Neelin, J. D.: Moisture vertical structure, column water vapor, and tropical deep convection, *Journal of the atmospheric sciences*, 66, 1665-1683, 2009.
- Jaenicke, R.: Aerosol physics and chemistry, *Landolt-Börnstein Neue Serie 4b*, 391-457, 1988.
- Jiang, H., Xue, H., Teller, A., Feingold, G., and Levin, Z.: Aerosol effects on the lifetime of shallow cumulus, *Geophysical Research Letters*, 33, 10.1029/2006gl026024, 2006.

- Jiang, H., Feingold, G., and Sorooshian, A.: Effect of aerosol on the susceptibility and efficiency of precipitation in warm trade cumulus clouds, *Journal of the Atmospheric Sciences*, 67, 3525-3540, 2010.
- Jiang, H. L., and Feingold, G.: Effect of aerosol on warm convective clouds: Aerosol-cloud-surface flux feedbacks in a new coupled large eddy model, *Journal of Geophysical Research-Atmospheres*, 111, D01202 10.1029/2005jd006138, 2006.
- Johnson, R. H., Rickenbach, T. M., Rutledge, S. A., Ciesielski, P. E., and Schubert, W. H.: Trimodal characteristics of tropical convection, *Journal of climate*, 12, 2397-2418, 1999.
- Kaufman, Y. J., Koren, I., Remer, L. A., Rosenfeld, D., and Rudich, Y.: The effect of smoke, dust, and pollution aerosol on shallow cloud development over the Atlantic Ocean, *Proceedings of the National Academy of Sciences of the United States of America*, 102, 11207-11212, 10.1073/pnas.0505191102, 2005.
- Khain, A. P., M. Ovchinnikov, M. Pinsky, A. Pokrovsky, and H. Krugliak: Notes on the state-of-the-art numerical modeling of cloud microphysics, *Atmos. Res.*, 55(3-4), 159-224, doi:10.1016/S0169-8095(00)00064-8, 2000.
- Khain, A., and Pokrovsky, A.: Simulation of effects of atmospheric aerosols on deep turbulent convective clouds using a spectral microphysics mixed-phase cumulus cloud model. Part II: Sensitivity study, *Journal of the Atmospheric Sciences*, 61, 2983-3001, 10.1175/jas-3281.1, 2004.
- Khain, A. P.: Notes on state-of-the-art investigations of aerosol effects on precipitation: a critical review, *Environmental Research Letters*, 4, 015004 (015020 pp.)-015004 (015020 pp.), 10.1088/1748-9326/4/1/015004, 2009.
- Khairoutdinov, M. F., and Randall, D. A.: Cloud resolving modeling of the ARM summer 1997 IOP: Model formulation, results, uncertainties, and sensitivities, *Journal of the Atmospheric Sciences*, 60, 2003.
- Kogan, Y. L., and Martin, W. J.: Parameterization of bulk condensation in numerical cloud models, *Journal of the atmospheric sciences*, 51, 1728-1739, 1994.
- Koren, I., Kaufman, Y. J., Remer, L. A., and Martins, J. V.: Measurement of the effect of Amazon smoke on inhibition of cloud formation, *Science*, 303, 1342-1345, 10.1126/science.1089424, 2004.
- Koren, I., Kaufman, Y. J., Rosenfeld, D., Remer, L. A., and Rudich, Y.: Aerosol invigoration and restructuring of Atlantic convective clouds, *Geophysical Research Letters*, 32, 10.1029/2005gl023187, 2005.
- Koren, I., Martins, J. V., Remer, L. A., and Afargan, H.: Smoke invigoration versus inhibition of clouds over the Amazon, *Science*, 321, 946-949, 10.1126/science.1159185, 2008.
- Koren, I., Oreopoulos, L., Feingold, G., Remer, L. A., and Altaratz, O.: How small is a small cloud?, *Atmos. Chem. Phys.*, 8, 3855-3864, 2008.
- Koren, I., Altaratz, O., Feingold, G., Levin, Z., and Reisin, T.: Cloud's Center of Gravity - a compact approach to analyze convective cloud development, *Atmospheric Chemistry and Physics*, 9, 155-161, 2009.
- Koren, I., Altaratz, O., Remer, L. A., Feingold, G., Martins, J. V., and Heiblum, R. H.: Aerosol-induced intensification of rain from the tropics to the mid-latitudes, *Nature Geoscience*, 2012.
- Koren, I., Dagan, G., and Altaratz, O.: From aerosol-limited to invigoration of warm convective clouds, *science*, 344, 1143-1146, 2014.
- Koren, I., Altaratz, O., and Dagan, G.: Aerosol effect on the mobility of cloud droplets, *Environmental Research Letters*, 10, 104011, 2015.
- Kuang, Z., and Bretherton, C. S.: A mass-flux scheme view of a high-resolution simulation of a transition from shallow to deep cumulus convection, *Journal of the Atmospheric Sciences*, 63, 1895-1909, 2006.
- Lee, S.-S., Feingold, G., and Chuang, P. Y.: Effect of aerosol on cloud-environment interactions in trade cumulus, *Journal of the Atmospheric Sciences*, 69, 3607-3632, 2012.

- Lee, S. S., Kim, B.-G., Lee, C., Yum, S. S., and Posselt, D.: Effect of aerosol pollution on clouds and its dependence on precipitation intensity, *Climate Dynamics*, 42, 557-577, 2014.
- Levin, Z., and Cotton, W. R.: *Aerosol pollution impact on precipitation: A scientific review*, Springer, 2009.
- Li, Z., Niu, F., Fan, J., Liu, Y., Rosenfeld, D., and Ding, Y.: Long-term impacts of aerosols on the vertical development of clouds and precipitation, *Nature Geoscience*, 4, 888-894, 10.1038/ngeo1313, 2011.
- Nitta, T., and Esbensen, S.: Heat and moisture budget analyses using BOMEX data, *Monthly Weather Review*, 102, 17-28, 1974.
- Pinsky, M., Mazin, I., Korolev, A., and Khain, A.: Supersaturation and diffusional droplet growth in liquid clouds, *Journal of the Atmospheric Sciences*, 70, 2778-2793, 2013.
- Roesner, S., Flossmann, A., and Pruppacher, H.: The effect on the evolution of the drop spectrum in clouds of the preconditioning of air by successive convective elements, *Quarterly Journal of the Royal Meteorological Society*, 116, 1389-1403, 1990.
- Rosenfeld, D.: TRMM observed first direct evidence of smoke from forest fires inhibiting rainfall, *Geophysical Research Letters*, 26, 3105-3108, 10.1029/1999gl006066, 1999.
- Rosenfeld, D.: Suppression of rain and snow by urban and industrial air pollution, *Science*, 287, 1793-1796, 10.1126/science.287.5459.1793, 2000.
- Rosenfeld, D., Lohmann, U., Raga, G. B., O'Dowd, C. D., Kulmala, M., Fuzzi, S., Reissell, A., and Andreae, M. O.: Flood or drought: How do aerosols affect precipitation?, *Science*, 321, 1309-1313, 10.1126/science.1160606, 2008.
- Saleeby, S. M., Herbener, S. R., van den Heever, S. C., and L'Ecuyer, T.: Impacts of Cloud Droplet–Nucleating Aerosols on Shallow Tropical Convection, *Journal of the Atmospheric Sciences*, 72, 1369-1385, 2015.
- Savane, O. S., Vant-Hull, B., Mahani, S., and Khanbilvardi, R.: Effects of Aerosol on Cloud Liquid Water Path: Statistical Method a Potential Source for Divergence in Past Observation Based Correlative Studies, *Atmosphere*, 6, 273-298, 2015.
- Seifert, A., and Heus, T.: Large-eddy simulation of organized precipitating trade wind cumulus clouds, *Atmos. Chem. Phys.*, 13, 5631-5645, 2013.
- Seifert, A., Heus, T., Pincus, R., and Stevens, B.: Large-eddy simulation of the transient and near-equilibrium behavior of precipitating shallow convection, *Journal of Advances in Modeling Earth Systems*, 2015.
- Seigel, R. B.: Shallow Cumulus Mixing and Subcloud Layer Responses to Variations in Aerosol Loading, *Journal of the Atmospheric Sciences*, 2014.
- Seiki, T., and Nakajima, T.: Aerosol effects of the condensation process on a convective cloud simulation, *Journal of the Atmospheric Sciences*, 71, 833-853, 2014.
- Siebesma, A. P., Bretherton, C. S., Brown, A., Chlond, A., Cuxart, J., Duynkerke, P. G., Jiang, H., Khairoutdinov, M., Lewellen, D., and Moeng, C. H.: A large eddy simulation intercomparison study of shallow cumulus convection, *Journal of the Atmospheric Sciences*, 60, 1201-1219, 2003.
- Small, J. D., Chuang, P. Y., Feingold, G., and Jiang, H.: Can aerosol decrease cloud lifetime?, *Geophysical Research Letters*, 36, 2009.
- Squires, P.: The microstructure and colloidal stability of warm clouds, *Tellus*, 10, 262-271, 1958.
- Squires, P., and Twomey, S.: The relation between cloud droplet spectra and the spectrum of cloud nuclei, *Geophysical Monograph Series*, 5, 211-219, 1960.
- Starr, J.: Some results of a trade-cumulus cloud investigation, *Journal of Meteorology*, 11, 220-237, 1954.
- Stevens, B.: On the growth of layers of nonprecipitating cumulus convection, *Journal of the atmospheric sciences*, 64, 2916-2931, 2007.
- Stevens, B., and Seifert, R.: Understanding macrophysical outcomes of microphysical choices in simulations of shallow cumulus convection, *Journal of the Meteorological Society of Japan*, 86, 143-162, 2008.

- Stevens, B., and Feingold, G.: Untangling aerosol effects on clouds and precipitation in a buffered system, *Nature*, 461, 607-613, 10.1038/nature08281, 2009.
- Takemi, T., Hirayama, O., and Liu, C.: Factors responsible for the vertical development of tropical oceanic cumulus convection, *Geophysical research letters*, 31, 2004.
- Tao, W.-K., Chen, J.-P., Li, Z., Wang, C., and Zhang, C.: Impact of aerosols on convective clouds and precipitation, *Reviews of Geophysics*, 50, RG2001, 2012.
- Trenberth, K. E., Fasullo, J. T., and Kiehl, J.: Earth's global energy budget, *Bull. Amer. Meteor. Soc.*, 90, 311-323, 2009.
- Waite, M. L., and Khouider, B.: The deepening of tropical convection by congestus preconditioning, *Journal of the Atmospheric Sciences*, 67, 2601-2615, 2010.
- Warner, J., and Twomey, S.: The production of cloud nuclei by cane fires and the effect on cloud droplet concentration, *Journal of the atmospheric Sciences*, 24, 704-706, 1967.
- Xue, H. W., and Feingold, G.: Large-eddy simulations of trade wind cumuli: Investigation of aerosol indirect effects, *Journal of the Atmospheric Sciences*, 63, 1605-1622, 10.1175/jas3706.1, 2006.
- Xue, H. W., Feingold, G., and Stevens, B.: Aerosol effects on clouds, precipitation, and the organization of shallow cumulus convection, *Journal of the Atmospheric Sciences*, 65, 392-406, 10.1175/2007jas2428.1, 2008.
- Yin, Y., K. S. Carslaw, and G. Feingold.: Vertical transport and processing of aerosols in a mixed-phase convective cloud and the feedback on cloud development. *Quarterly Journal of the Royal Meteorological Society* 131.605 221-245, 2005.
- Yuan, T., Remer, L. A., and Yu, H.: Microphysical, macrophysical and radiative signatures of volcanic aerosols in trade wind cumulus observed by the A-Train, *Atmospheric Chemistry and Physics*, 11, 7119-7132, 10.5194/acp-11-7119-2011, 2011.
- Zhao, M., and Austin, P. H.: Life cycle of numerically simulated shallow cumulus clouds. Part I: Transport, *Journal of the Atmospheric Sciences*, 62, 1269-1290, 10.1175/jas3414.1, 2005.
- Zuidema, P., Li, Z., Hill, R. J., Bariteau, L., Rilling, B., Fairall, C., Brewer, W. A., Albrecht, B., and Hare, J.: On trade wind cumulus cold pools, *Journal of the Atmospheric Sciences*, 69, 258-280, 2012.



Formatted: Font: (Default) +Headings CS (Times New Roman), 12 pt, Complex Script
Font: +Headings CS (Times New Roman), 12 pt

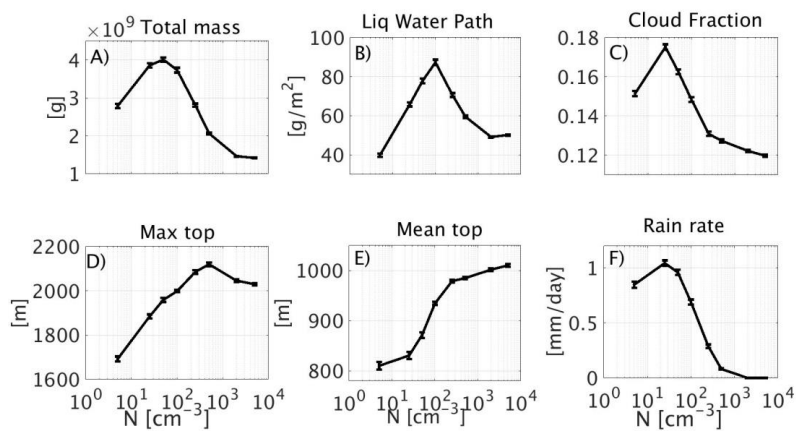
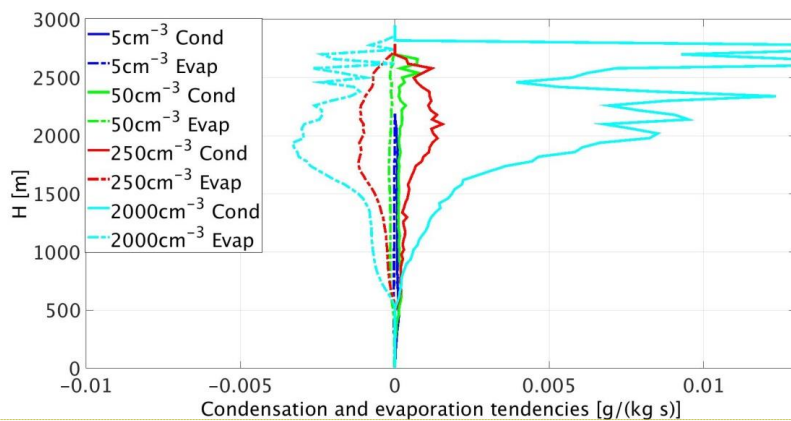
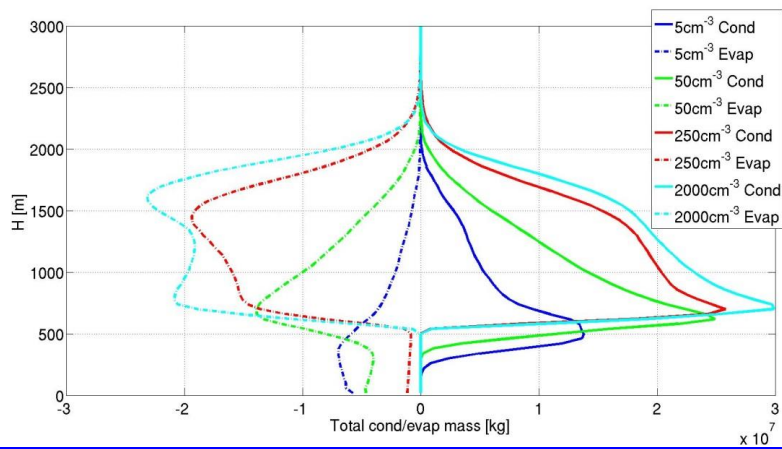


Figure 2. mean properties (over domain and time) of the simulated cloud fields as a function of the aerosol concentration used in the simulation: A) total liquid water mass in the domain, B) cloudy LWP, C) cloud fraction (CF) for columns with $\tau > 0.3$, D) maximum cloud top, E) mean cloud top, and, F) surface rain rate. Each of these mean properties are calculated for the last 14 hours out of the 16 hours of simulation. The error bars present the standard errors. For details about the different properties see the text.

Formatted: Font: (Default) +Headings CS (Times New Roman), 10 pt, Bold, Complex Script Font: +Headings CS (Times New Roman), 10 pt, Bold



Formatted: Font: (Default) +Headings CS (Times New Roman), 10 pt, Bold, Complex Script Font: +Headings CS (Times New Roman), 10 pt, Bold



Formatted: Font: (Default) +Headings CS (Times New Roman), 12 pt, Bold, Complex Script Font: +Headings CS (Times New Roman), 12 pt, Bold

Figure 2. Domain's mean total condensation (solid lines) and evaporation mass tendencies for 14 hours of simulation for along four different simulations conducted with different aerosol concentration levels (5 cm^{-3} blue, 50 cm^{-3} green, 250 cm^{-3} red and 2000 cm^{-3} cyan).

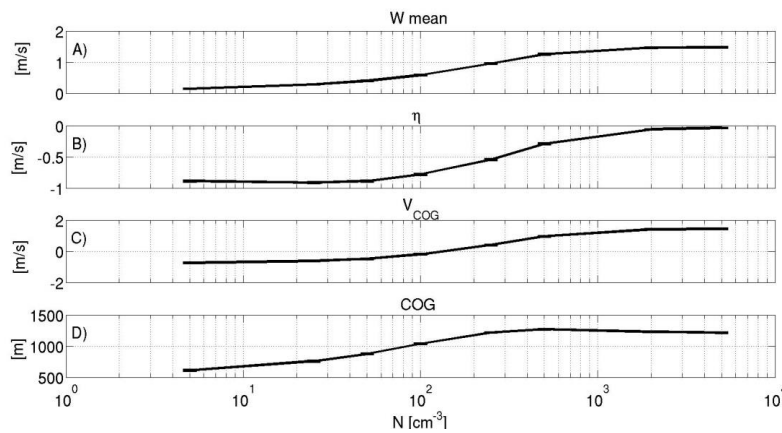


Figure 3. Mean (over time and space) of A) updraft (W), B) effective terminal velocity (η), C) the center of gravity velocity V_{COG} and D) COG (center of gravity) height as a function of the aerosol concentration. All calculated for the last 14 hours out of the 16 hours of simulation.

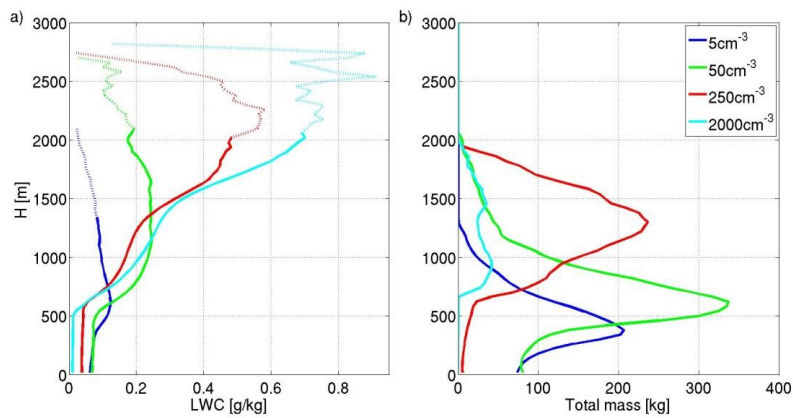
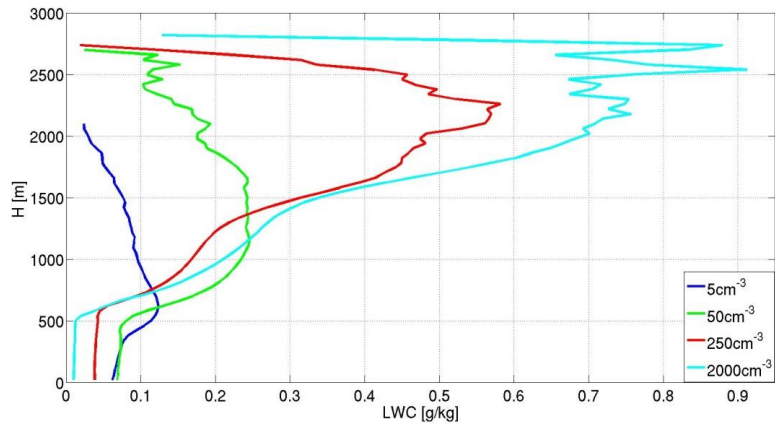


Figure 4. a) Mean liquid water content (LWC) vertical profiles for four different simulations (5 cm^{-3} blue, 50 cm^{-3} green, 250 cm^{-3} red and 2000 cm^{-3} cyan). b) Vertical profiles of the mean (over time) total liquid water mass per height for four different simulations (5 cm^{-3} blue, 50 cm^{-3} green, 250 cm^{-3} red and 2000 cm^{-3} cyan). The mean profiles are calculated for the last 14 hours out of the 16 hours of simulation. Note that Dotted parts of the curves in a) represents heights in which the total liquid water mass was less than 1% of the maximum total mass (Fig. 4b).

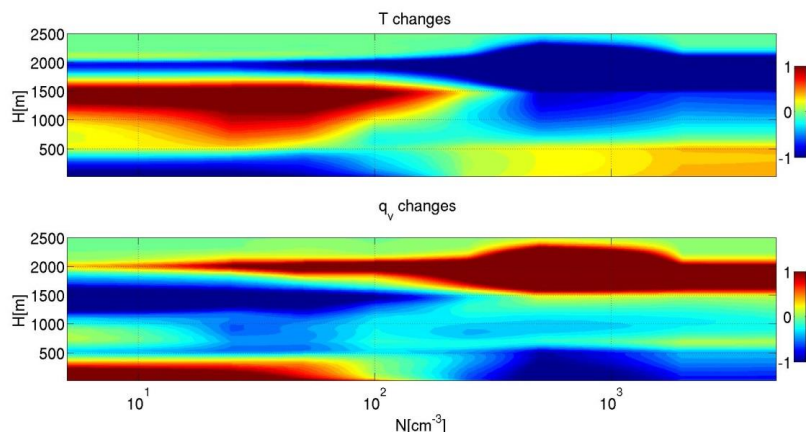
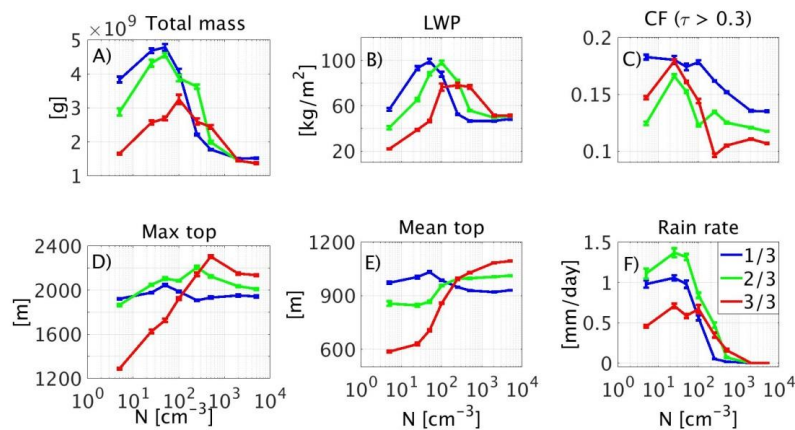


Figure 5. Total change, during 16 h of simulation in the temperature ([k] upper panel) and water vapor content ([g/kg] – lower panel) domain mean vertical profiles as a function of the aerosol concentration used in the simulation.



Formatted: Font: (Default) +Headings CS (Times New Roman), 10 pt, Bold, Complex Script Font: +Headings CS (Times New Roman), 10 pt, Bold

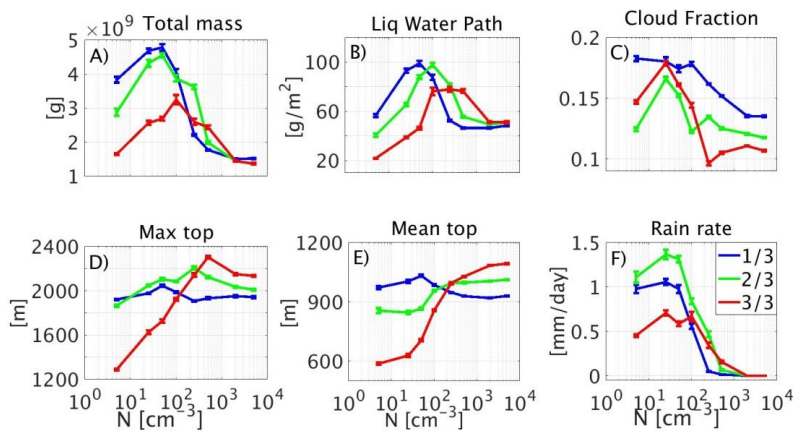


Figure 6. Mean properties (over time and domain) of the simulated cloud fields as a function of the aerosol concentration used in the simulation: A) total liquid water mass in the domain, B) cloudy LWP, C) cloud fraction (CF) for columns with $\tau > 0.3$, D) maximum cloud top, E) mean cloud top, and, F) surface rain rate. Each property is calculated separately for each period of one third of the simulations (blue, green and red for the first, second and third periods, respectively). The error bars present the standard error. For details about the different properties, see the text.

Table 1. change (in %) in key variables between the mean values in the last third period of the simulations and the first period. Negative values are presented in red.

	Total mass [%]	LWP [%]	COG [%]	Max top [%]	Mean top [%]	W max [%]	CF [%]	Rain rate [%]
5 cm ⁻³	-57.0	-61.4	-43.1	-32.9	-39.7	-28.2	-19.7	-53.5
25 cm ⁻³	-45.2	-58.3	-39.6	-17.8	-37.4	-38.8	-0.6	-32.9
50 cm ⁻³	-43.8	-53.1	-33.7	-15.6	-31.6	-47.9	-7.5	-40.1
100 cm ⁻³	-20.1	-13.0	-16.1	-3.2	-13.0	-32.8	-19.0	19.6
250 cm ⁻³	17.5	48.6	5.0	12.4	5.0	-4.3	-40.7	598.1
500 cm ⁻³	37.4	64.2	19.9	19.2	10.7	9.4	-30.9	841.5
2000 cm ⁻³	-3.7	10.6	14.8	10.1	17.9	6.0	-17.8	-
5000 cm ⁻³	-10.1	5.7	13.7	9.9	17.5	2.9	-20.7	-

Formatted: Font: (Default) +Headings CS (Times New Roman), 10 pt, Bold, Complex Script Font: +Headings CS (Times New Roman), 10 pt, Bold

